

# Supramolecular Association of Pyrrolidinofullerenes Bearing Chelating Pyridyl Groups and Zinc Phthalocyanine for Organic Solar Cells

Pavel A. Troshin,<sup>\*,†</sup> Robert Koeppe,<sup>\*,‡</sup> Alexander S. Peregudov,<sup>§</sup> Svetlana M. Peregudova,<sup>§</sup> Martin Egginger,<sup>‡</sup> Rimma N. Lyubovskaya,<sup>†</sup> and N. Serdar Sariciftci<sup>‡</sup>

*Institute of Problems of Chemical Physics of RAS, Chernogolovka, Moscow Region, 142432, Russia, Linz Institute for Organic Solar Cells (LIOS), Johannes Kepler University Linz, Altenbergerstrasse 69, A-4040 Linz, Austria, and A. N. Nesmeyanov Institute of Organoelement Compounds, Vavilova St. 28, B-334, Moscow, 119991, Russia*

Received May 8, 2007. Revised Manuscript Received August 7, 2007

We investigated donor–acceptor bilayer heterojunctions formed by deposition of solution-processed pyrrolidinofullerenes bearing chelating pyridyl groups (PyFs) on vacuum-evaporated films of zinc phthalocyanine (ZnPc). It is shown that coordination complexes are formed at the interface between these donor and acceptor components; such association facilitates photoinduced charge separation and results in improved performance of the photovoltaic devices. Thus, the bilayer photovoltaic cells fabricated from different pyrrolidinofullerenes and ZnPc exhibit short circuit current ( $I_{sc}$ ) densities in the range of 3–5 mA/cm<sup>2</sup>, open circuit voltages ( $V_{oc}$ ) of 400–600 mV, and fill factors (FF) of 40–50% that correspond to power conversion efficiencies ( $\eta$ ) of up to 1.5% under 100 mW/cm<sup>2</sup> simulated AM1.5 illumination. The reference cells based on the nonchelating fullerene derivative [6,6]-phenyl-C<sub>61</sub> butyric acid methyl ester (PCBM) as acceptor component yield lower power conversion efficiencies (0.4–0.6%); the performance of such devices can be increased significantly by mixing PCBM with a small amount (4% w/w) of PyF in the acceptor layer. A novel multicomponent organic solar cell architecture is suggested in order to expand the active layer absorption by formal combination of the solution-processed bulk heterojunction polymer/fullerene cells with evaporated bilayer ZnPc/fullerene devices. For this purpose, a blend of the fullerene derivatives (PCBM and PyF mixed in different ratios) with the polyconjugated polymer poly((2-methoxy-5-(3,7-dimethyloctyloxy)-*p*-phenylene) vinylene (MDMO–PPV) is spin-coated on the ZnPc film sublimed on an indium tin oxide (ITO) substrate. Evaporation of the top aluminum electrodes yields photovoltaic devices that demonstrate power conversion efficiencies of up to 2% and efficient photocurrent generation in the full range from 350 to 820 nm.

## 1. Introduction

Many research efforts are focused on the development of low-cost flexible organic solar cells using fullerenes or their derivatives as acceptor components.<sup>1–3</sup> The two main concepts in the design of organic solar cells consist of blending donor and acceptor components together in solution and casting into thin films to yield “bulk heterojunction” type devices,<sup>4,5</sup> whereas the other route is based on thermal evaporation/sublimation of the small molecular semiconductors as thin films on a substrate in high vacuum.<sup>6,7</sup>

The basic working principle of organic solar cells is the dissociation of photogenerated excitations at the interface between electron donor and acceptor phases by a photoinduced charge-transfer process with subsequent transport of the charge carriers in the respective phases to the electrodes.<sup>8</sup> Critical parameters for the photocurrent generation are therefore the active layer absorption, the efficiency of the charge transfer, and the transport of charge carriers in the materials involved.

A severe limitation for the efficiency of the bulk heterojunction devices is a relatively narrow absorption spectrum. Thus, the best solar cells made from the polyconjugated polymer poly(2-methoxy-5-{3',7'-dimethyloctyloxy}-*p*-phenylene vinylene) (MDMO–PPV) and 1-(3-methoxycarbonyl)propyl-1-phenyl[6,6]C<sub>61</sub> (PCBM) demonstrate power conversion efficiencies of 2.5% under AM1.5 conditions.<sup>9</sup> Even better suited for building solar cells is a combination of PCBM with regioregular poly(3-hexylthiophene) (P3HT), which possesses better hole transport properties and a

<sup>†</sup> Institute of Problems of Chemical Physics of RAS.

<sup>‡</sup> Johannes Kepler University Linz.

<sup>§</sup> A. N. Nesmeyanov Institute of Organoelement Compounds.

- (1) Shaheen, S. E.; Ginley, D. S.; Jabbour, G. E. *MRS Bull.* **2005**, *30*, 10.
- (2) Hoppe, H.; Sariciftci, N. S. *J. Mater. Res.* **2004**, *19*, 1924.
- (3) Hoppe, H.; Sariciftci, N. S. *J. Mater. Chem.* **2006**, *16*, 45.
- (4) Yu, G.; Gao, J.; Hummelen, J. C.; Wudl, F.; Heeger, A. J. *Science* **1995**, *270*, 1789.
- (5) Halls, J. J. M.; Walsh, C. A.; Greenham, N. C.; Marsaglia, E. A.; Friend, R. H.; Moratti, S. C.; Holmes, A. B. *Nature* **1995**, *376*, 498.
- (6) (a) Tang, C. W. *Appl. Phys. Lett.* **1986**, *48*, 183. (b) Schulze, K.; Urich, C.; Schuppel, R.; Leo, K.; Pfeiffer, M.; Brier, E.; Reinold, E.; Bauerle, P. *Adv. Mater.* **2006**, *18*, 2872.
- (7) Wöhrle, D.; Meissner, D. *Adv. Mater.* **1991**, *3*, 129.

(8) Sariciftci, N. S.; Smilowitz, L.; Heeger, A. J.; Wudl, F. *Science* **1992**, *258*, 1474.

(9) Shaheen, S. E.; Brabec, C. J.; Sariciftci, N. S.; Padinger, F.; Fromherz, T.; Hummelen, J. C. *Appl. Phys. Lett.* **2001**, *78*, 841.

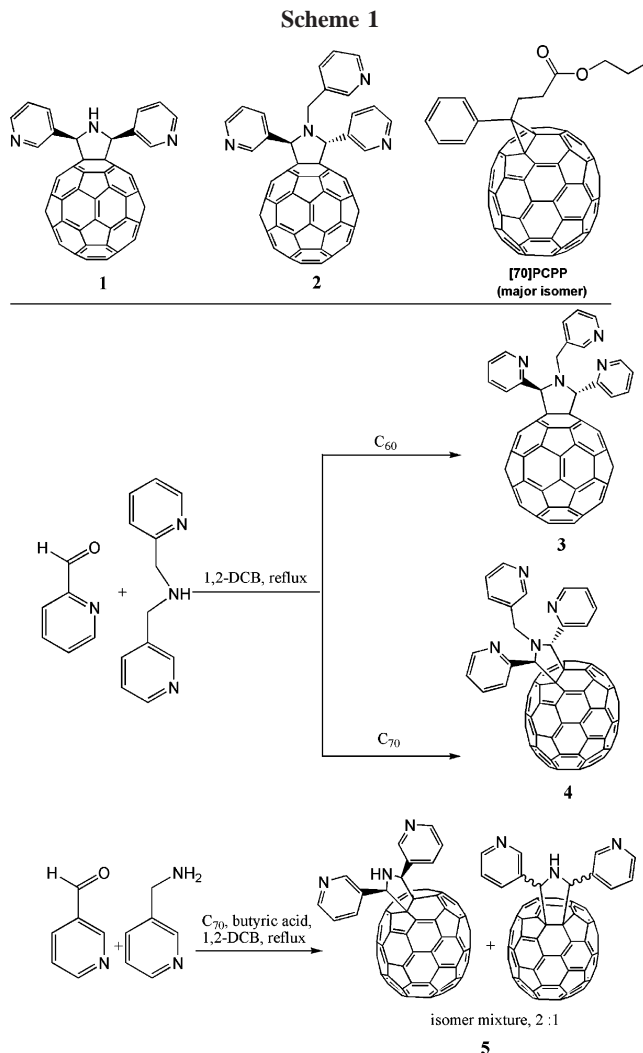
significantly wider absorption spectrum (up to  $\sim 650$  nm) than MDMO-PPV.<sup>10</sup> Therefore, the optimization of the active layer morphology of P3HT-PCBM solar cells resulted in power conversion efficiencies of 4–5% reported recently by several independent groups.<sup>11,12</sup> However, this value seems to be very close to the theoretical maximum determined by the optoelectronic properties of these donor and acceptor materials.<sup>13</sup>

An intensively investigated route for improvement of organic photovoltaics is the development of low band gap donor polymers that absorb the light in the red and infrared spectral regions. However, most available low band gap polymers yield solar cells with power conversion efficiencies below 1.5%;<sup>14–17</sup> only very recently two examples of low band gap polymers that yielded power conversion efficiencies as high as 2.2% and 3.2% were presented.<sup>18,19</sup> Generally, lower charge carrier mobilities and higher lying HOMO energy levels of the donor decreasing the  $V_{oc}$  are major disadvantages of low energy gap polymers.<sup>20,21</sup>

The chemical attachment of chromophore units such as phthalocyanines, perylene diimides, and cyanine dyes to the fullerene cage yields electron acceptor materials that absorb the light in a wider spectral region. However, the evaluation of such compounds in organic solar cells demonstrated very low power conversion efficiencies (0.01–0.2%) most probably related to poor charge carrier transport in these materials.<sup>22–24</sup>

Thermal evaporation of materials for photovoltaic devices is a technique suggested long before the solution-based bulk heterojunction approach.<sup>6,7</sup> Pristine [60]fullerene and metal phthalocyanines (such as ZnPc and CuPc) are the materials of choice for this type of solar cell that can yield high power conversion efficiencies (2–4%).<sup>25–27</sup>

We recently presented the application of a solution-processed fullerene derivative as the acceptor component in



diffuse bilayer devices in combination with zinc phthalocyanine (ZnPc).<sup>28</sup> The presence of chelating pyridyl groups in the molecular framework of the fullerene-based acceptor (termed PyF) coordinate with the metal center in the donor ZnPc; such a supramolecular association was shown in solution and occurs during the deposition of the fullerene solution onto the evaporated ZnPc film at the interface between these two materials.<sup>29</sup> It was suggested that this complex formation facilitates the photoinduced charge separation process and improves the performance of the PyF/ZnPc photovoltaic devices.

In this paper we report on the preparation of several different fullerene-based materials bearing chelating pyridyl groups (PyFs, Scheme 1), with a comparative investigation of their interactions with ZnPc in solid thin films and evaluation of the performance of these materials in bilayer organic solar cells. To achieve efficient photocurrent generation in a wide spectral region, we merged bulk heterojunction MDMO-PPV/PCBM cells and bilayer ZnPc/PyF cells in a multicomponent device structure.

- (10) Buvat, P.; Hourquebie, P. *Macromolecules* **1997**, *30*, 2685.  
 (11) Reyes-Reyes, M.; Kim, K.; Carrola, D. L. *Appl. Phys. Lett.* **2005**, *87*, 083506.  
 (12) Reyes-Reyes, M.; Kim, K.; Carroll, D. L.; Dewald, J.; Lopez-Sandoval, R.; Avadhanula, A.; Curran, S.; Carroll, D. L. *Org. Lett.* **2005**, *7*, 5749.  
 (13) Scharber, M. C.; Muhlbacher, D.; Koppe, M.; Denk, P.; Waldauf, C.; Heeger, A. J.; Brabec, C. J. *Adv. Mater.* **2006**, *18*, 789.  
 (14) Wang, X.; Perzon, E.; Oswald, F.; Langa, F.; Admassie, S.; Andersson, M. R.; Inganäs, O. *Adv. Funct. Mater.* **2005**, *15*, 1665.  
 (15) Campos, L. M.; Tontcheva, A.; Gunes, S.; Sonmez, G.; Neugebauer, H.; Sariciftci, N. S.; Wudl, F. *Chem. Mater.* **2005**, *17*, 4031.  
 (16) Wienk, M. M.; Turbiez, M. G. R.; Struijk, M. P.; Fonrodona, M.; Janssen, R. A. J. *Appl. Phys. Lett.* **2006**, *88*, 153511.  
 (17) Shi, C.; Yao, Y.; Yang, Y.; Pei, Q. *J. Am. Chem. Soc.* **2006**, *128*, 8980.  
 (18) Zhang, F.; Mammo, W.; Andersson, L. M.; Admassie, S.; Andersson, M. R.; Inganäs, O. *Adv. Mater.* **2006**, *18*, 2169.  
 (19) Muhlbacher, D.; Scharber, M.; Morana, M.; Zhu, Z.; Waller, D.; Gaudiana, R.; Brabec, C. *Adv. Mater.* **2006**, *18*, 2884.  
 (20) Andersson, M.; Inganäs, O. *Appl. Phys. Lett.* **2006**, *88*, 082103.  
 (21) Koster, L. J. A.; Mihailetschi, V. D.; Blom, P. W. M. *Appl. Phys. Lett.* **2006**, *88*, 093511.  
 (22) Loi, M. A.; Denk, P.; Hoppe, H.; Neugebauer, H.; Winder, C.; Meissner, D.; Brabec, C.; Sariciftci, N. S.; Gouloumis, A.; Vazquez, P.; Torres, T. *J. Mater. Chem.* **2003**, *13*, 700.  
 (23) Meng, F.; Hua, J.; Chen, K.; Tian, H.; Zuppiroli, L.; Nuesch, F. *J. Mater. Chem.* **2005**, *15*, 979.  
 (24) Hua, J.; Meng, F.; Ding, F.; Li, F.; Tian, H. *J. Mater. Chem.* **2004**, *14*, 1849.  
 (25) Peumans, P.; Forrest, S. R. *Appl. Phys. Lett.* **2001**, *79*, 126.  
 (26) Forrest, S. R. *MRS Bull.* **2005**, *30*, 28.  
 (27) Gebeyehu, D.; Pfeiffer, M.; Maennig, B.; Drechsel, J.; Werner, A.; Leo, K. *Thin Solid Films* **2004**, *451*, 29.

- (28) Koeppe, R.; Troshin, P. A.; Lyubovskaya, R. N.; Sariciftci, N. S. *Appl. Phys. Lett.* **2005**, *87*, 244102.  
 (29) Koeppe, R.; Troshin, P. A.; Fuchsbaue, A.; Lyubovskaya, R. N.; Sariciftci, N. S. *Fullerenes, Nanotubes, Carbon Nanostruct.* **2006**, *14*, 441.

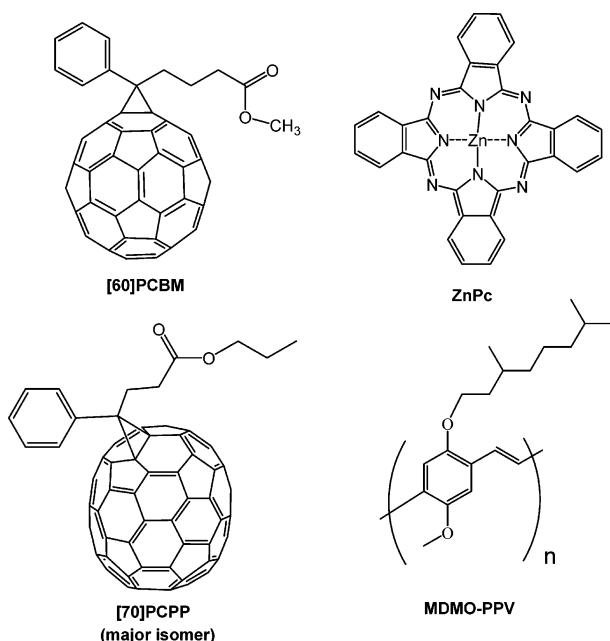


**Figure 1.** Molecular structure of non-pyrrolidinofullerene materials used in this work.

## 2. Results and Discussion

**Synthesis of Materials.** The pyrrolidinofullerenes **1** and **2** were synthesized according to the method reported previously;<sup>30</sup> [70]PCPP was prepared starting from C<sub>70</sub> and tosylhydrazone of methyl ester of phenylpropionic acid according to the procedure reported previously for [70]-PCBM.<sup>31</sup> New pyrrolidinofullerene compounds **3–5** were prepared as outlined in Scheme 1. All new compounds were fully characterized by 1D <sup>1</sup>H and <sup>13</sup>C NMR (see the Experimental Section); the assignment of cis and trans configurations of substituents in the pyrrolidine ring of these compounds was performed using 2D NOESY (nuclear Overhauser enhancement spectroscopy) experiments and will be described in detail separately.<sup>32</sup>

The molecular structures of commercially available materials used in this work are shown in Figure 1.

**Cyclic Voltammetry Study of PyFs 1–5.** In order to compare the acceptor strength of the fullerene derivatives used in this work, we studied their electrochemical reduction in 1,2-dichlorobenzene solution using cyclic voltammetry. The determined reduction potentials are given in Table 1. All derivatives of [60]fullerene exhibit three reversible reductions, while the fourth reduction wave was irreversible. On the contrary, compounds with C<sub>70</sub> core undergo four reversible reductions; the larger  $\pi$ -system of [70]fullerene derivatives makes the formation of stable tetraanions possible.

The first reduction potentials of all compounds are very close or even equal to  $E_{1/2}^1$  of [60]PCBM, a widely used material for organic solar cells. It means that all fullerene-

**Table 1.** Reduction Potentials ( $E_{1/2}$ ) of the Studied Fullerene Derivatives vs SCE Determined from Cyclic Voltammetry Measurements

compd	$E_{1/2}$ , V vs SCE			
	$E_{1/2}^1$	$E_{1/2}^2$	$E_{1/2}^3$	$E_{1/2}^4$
<b>1</b>	-0.74	-1.14	-1.67	
<b>2</b>	-0.76	-1.17	-1.71	
<b>3</b>	-0.78	-1.18	-1.73	
<b>4</b>	-0.78	-1.18	-1.57	-2.04
<b>5</b>	-0.75	-1.15	-1.53	-1.94
[70]PCPP	-0.76	-1.18	-1.6	-2.12
[60]PCBM	-0.78	-1.21	-1.77	

based materials studied here have similar LUMO (lowest unoccupied molecular orbital) energy levels. The energy difference between the acceptor LUMO and donor HOMO (highest occupied molecular orbital) levels determines the maximal  $V_{oc}$  value that can be achieved in an organic solar cell based on a given pair of donor and acceptor materials.<sup>13,33</sup> Thus, the investigated fullerene derivatives should allow similar  $V_{oc}$  values in organic solar cells.

Surprisingly, the values of the third and fourth reduction potentials of the compounds depend quite strongly on the composition and structure of organic groups attached to the fullerene cage. It seems that these organic addends participate somehow in the charge stabilization together with the fullerene  $\pi$ -system when fullerene derivatives are reduced to tri- and tetraanions.

### Complexation of the Fullerene Derivatives with ZnPc.

The samples prepared by spin-coating fullerene derivatives **1–5** and PCBM as a reference compound on the ZnPc films exhibited significantly different absorption profiles (Figure 2). The absorption spectrum of the reference sample comprising PCBM–ZnPc corresponds to the superposition of the absorption spectra of the individual components with an additional broad band appearing at 430–520 nm. The absorption of the pristine materials is rather weak in this region; therefore, the observed band indicates additional electronic interactions appearing as a result of the deposition of PCBM onto the ZnPc film. Additional bands (that will be termed “interaction bands” below) with different intensities were also observed in the spectra of ZnPc films covered with PyFs **1** (maximum at 405 nm), **2** (455 nm), **3** (~450 nm), **4** (490 nm), and **5** (450 nm) that reflects a similar behavior of all studied fullerene derivatives. It should be noted that no additional bands in this spectral area were reported when C<sub>60</sub> was combined with ZnPc by sequential vacuum deposition of thin films or using a coevaporation technique.<sup>34,35</sup>

The exact origin of the observed interaction bands is yet unknown. Perhaps they arise from a symmetry breaking due to association of ZnPc on the spherical fullerenes, as observed in less symmetrical fullerenes like C<sub>70</sub>.<sup>36</sup>

(30) Troshin, P. A.; Peregodov, A. S.; Muhlbacher, D.; Lyubovskaya, R. N. *Eur. J. Org. Chem.* **2005**, *14*, 3064.

(31) Wienk, M. M.; Kroon, J. M.; Verhees, W. J. H.; Knol, J.; Hummelen, J. C.; van Hall, P. A.; Janssen, R. A. J. *Angew. Chem., Int. Ed.* **2003**, *42*, 337.

(32) Troshin, P. A.; Peregodov, A. S.; Peregodova, S. M.; Lyubovskaya, R. N., to be submitted for publication.

(33) Brabec, C. J.; Cravino, A.; Meissner, D.; Sariciftci, N. S.; Fromherz, T.; Rispen, M. T.; Sanchez, L.; Hummelen, J. C. *Adv. Funct. Mater.* **2001**, *11*, 374.

(34) Drechsel, J.; Mannig, B.; Kozlowski, F.; Gebeyehu, D.; Werner, A.; Koch, M.; Leo, K.; Pfeiffer, M. *Thin Solid Films* **2004**, *451–452*, 515.

(35) Pannemann, Ch.; Dyakonov, V.; Parisi, J.; Hild, O.; Wöhrle, D. *Synth. Met.* **2001**, *121*, 1585.

(36) Kazaoui, S.; Minami, N.; Tanabe, Y.; Byrne, H. J.; Eilmel, A.; Petelenz, P. *Phys. Rev. B* **1998**, *58*, 7689.

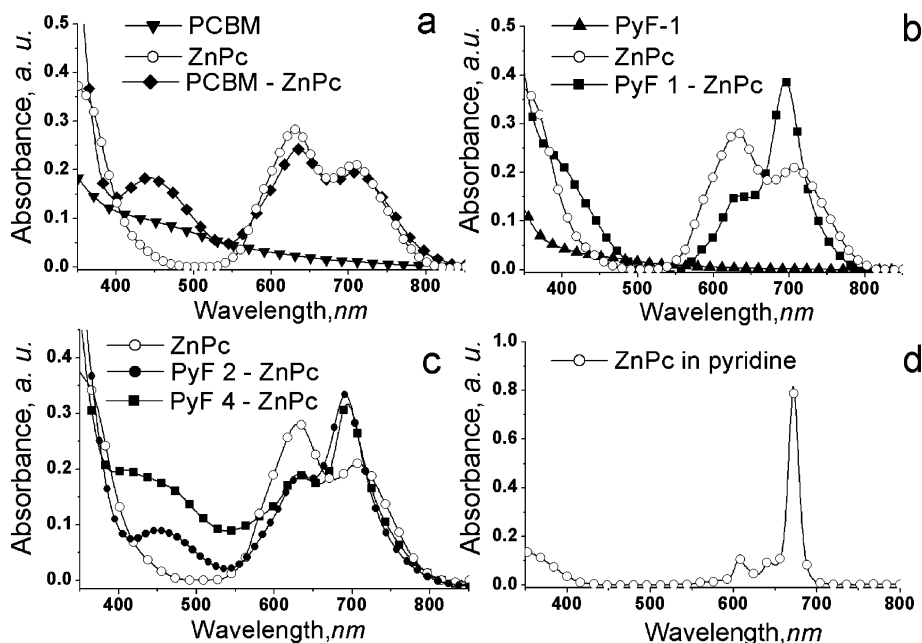


**Figure 2.** Absorption spectra of the ZnPc-PCBM (a) and ZnPc-PyF-1 (b) systems shown in comparison with the normalized spectra of the pristine materials. Changes in the absorption profile of ZnPc films covered with different fullerene derivatives (c); solution-state absorption spectrum of ZnPc (d).

The coordination complex formation between PyFs 1–5 and ZnPc results in pronounced spectral changes in the phthalocyanine Q-band between 550 and 800 nm. The absorption spectrum of the solid film of pristine ZnPc has two maxima at ca. 630 and 712 nm, whereas the solution spectrum of this material is characterized mainly by a single sharp Q-band at 674 nm. Spin-coating the compounds 1–5 on the ZnPc film results in the appearance of sharp bands with maxima at 690–694 nm that are quite similar to the absorption spectrum of the phthalocyanine in solution (Figure 2d). The strongest changes in the absorption spectra were observed for the ZnPc films covered with PyF-1 (Figure 2), a much weaker effect was caused by compounds 2 and 4, and the least pronounced change was induced by PyF-3 and PyF-5. The complexation of the ZnPc unit with the fullerene derivative most probably results in the disturbance of the stacking of the phthalocyanine  $\pi$ -system with neighboring ZnPc molecules; similarly, in solution the ZnPc units are separated by the solvent molecules.

A system composed of a soluble zinc naphthalocyanine derivative and a fullerene compound possessing chelating groups was investigated previously in solutions.<sup>37</sup> However, in this case absorption spectroscopy did not reveal pronounced spectral changes upon the complex formation as we observed here for the complexation in solid state. The absorption changes are due to a perturbation of the interaction between the metal complexes in the solid state due to the introduction of the complexing fullerenes.

**Diffused Bilayer Organic Solar Cells Fabricated from PyFs 1–5 and ZnPc.** The schematic solar cell structure is shown in Figure 3. The solar cell output parameters were reproduced within at least 30 devices for each system; the obtained values are given in Table 2 (measurements under 100 mW/cm<sup>2</sup> simulated AM1.5 illumination). It can be

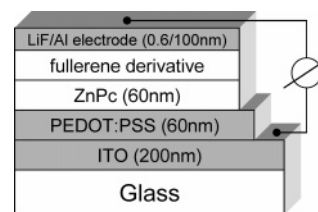


**Figure 3.** Schematic layout of the investigated diffuse bilayer solar cell architecture.

**Table 2. Output Parameters of Bilayer Solar Cells Fabricated Using Different Acceptor Materials**

composition of the acceptor layer	$I_{sc}$ (mA/cm <sup>2</sup> )	$V_{oc}$ (mV)	FF (%)	$\eta$ (%)
PyF-1	2.8–3.3	370–450	40–45	0.4–0.6
PyF-2	3.5–3.9	420–460	46–52	0.7–0.9
PyF-3	3.6–4.9	550–620	45–52	0.9–1.5
PyF-4	2.8–3.1	520–560	38–49	0.6–0.9
PyF-5	3.1–3.5	440–490	43–48	0.6–0.8
PCBM	2.2–2.8	380–460	46–61	0.4–0.7
96% PCBM + 4% PyF-2	3.5–3.8	470–520	45–51	0.8–1.0
96% PCBM + 4% PyF-3	3.4–4.5	520–540	47–50	0.8–1.2

derived from this data that solar cells fabricated with the PyFs 1–5 yield significantly higher currents than the reference devices with PCBM. The highest short circuit current densities ( $I_{sc} = 4.9$  mA/cm<sup>2</sup>) and open circuit voltages ( $V_{oc} = 600$  mV) were obtained for solar cells with compound 3 that give power conversion efficiencies of  $\sim 1.5\%$ . The typical light  $I$ - $V$  characteristics for solar cells with several different fullerene materials cast on ZnPc are shown in Figure 4.

The incident photon to collected electron efficiency (IPCE) spectra of typical devices built using PyF-2, PyF-3, and PCBM as acceptor materials are shown in Figure 5. All three spectra are very similar below  $\sim 420$  nm where the fullerene absorption gives the major contribution to the IPCE. The IPCE spectra are the most distinct in the range of 550–850 nm, where pristine ZnPc films show the strongest absorption. Thus, PyF-3/ZnPc solar cells demonstrate at least 2 times

(37) El-Khouly, M. E.; Rogers, L. M.; Zandler, M. E.; Suresh, G.; Futjitsuka, M.; Ito, O.; D'Souza, F. *ChemPhysChem* **2003**, *4*, 474.

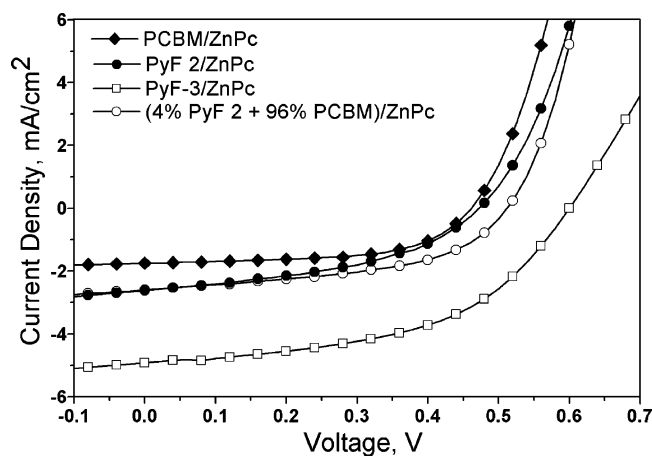


**Figure 4.** Linear  $I$ - $V$  curves for solar cells with acceptor materials comprising PCBM, PyF-2, and 96% PCBM + 4% PyF-2 w/w mixture under  $100 \text{ mW/cm}^2$  AM1.5 illumination.

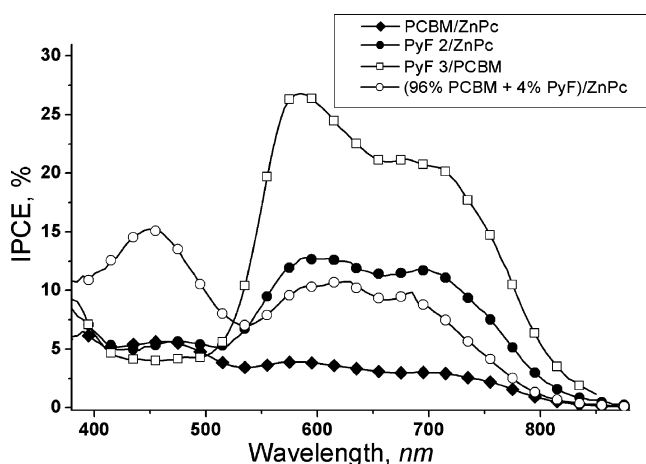


**Figure 5.** Typical IPCE spectra for solar cells made from ZnPC and different acceptor materials; PCBM is compared with PyF-2 and mixture PCBM-PyF-2 96:4 (w/w).

and 6–7 times higher IPCE values than PyF-2/ZnPC and PCBM/ZnPC devices, respectively. The enhanced participation of the phthalocyanine in the photocurrent generation seems to be related to its association with PyF; a tight electronic communication between the components in such complexes can provide an efficient pathway for charge carrier generation.

The efficiency of PCBM-ZnPC solar cells can be significantly improved by the introduction of small amounts of pyrrolidinofullerenes into the photoactive layer. This was achieved by spin-coating mixtures of 4% pyrrolidinofullerene (PyF-2 or PyF-3, Table 2) and 96% PCBM from dichloromethane solutions onto the ZnPC films. The corresponding photovoltaic devices yielded short circuit current densities ( $I_{sc}$ ) of 3.5–4.5  $\text{mA/cm}^2$  (Table 2). This means that an addition of very small amounts of PyF into the PCBM solution can double the photocurrent yield. We propose a specific and effective electronic interaction between ZnPC and PyF, such as organometallic coordination between the pyrrolidines of the fullerenes and metal center of the phthalocyanines. Moreover, the combination of PCBM with PyFs increases the open circuit voltage ( $V_{oc}$ ) up to 540 mV for the PyF-3-PCBM system.

The effect of addition of 4% of PyF-2 to PCBM on the photocurrent is especially evident from the IPCE spectra shown in Figure 5. Notable is the presence of an intense feature at 400–530 nm in the IPCE spectrum of the PCBM-PyF-2-ZnPC devices. The absorption of pristine materials is rather weak in this region; therefore, the interaction bands appearing in the absorption of ZnPC films covered with PCBM and PyF-2 (Figure 2c) contribute to the photocurrent generation. The same band is present in the IPCE spectrum of ZnPC-PCBM devices, though the overall magnitude of the photocurrent is much lower as compared to PCBM-PyF-2-ZnPC cells.

The increased performance of PyF-ZnPC solar cells as compared to the PCBM-ZnPC devices can arise either from better electron transport properties of compounds 1–5 with respect to PCBM or from an improved charge carrier generation in the PyF-ZnPC donor-acceptor system. The former is unlikely since PyF/ZnPC solar cells give lower fill factors (FF) than PCBM/ZnPC devices. We propose that the photoinduced charge separation is facilitated in the PyF-ZnPC systems due the coordination complex formation between these materials. The existence of coordination bonds between the ZnPC and PyF could significantly lower the activation energy barrier of the photoinduced electron transfer as was observed previously for many studied PyF-Zn-porphyrin dyads.<sup>38</sup>

It was reported previously that the application of  $C_{70}$ -based material ( $C_{70}$ -PCBM) in bulk heterojunction solar cells results in a ca. 1.5-fold increase in the current densities ( $I_{sc}$ ) over analogous  $C_{60}$ -PCBM devices. This effect is attributed to a stronger visible absorption of  $C_{70}$  derivatives in comparison with their  $C_{60}$  relatives. However, we observed no such clear effect in the devices when PyFs 1, 2, or 3 were replaced by  $C_{70}$  derivatives 4 and 5. Particularly, the differences in the absorption spectra (Figure 2c) of ZnPC films covered with PyFs 1–5 are not significant enough to expect any increase in the photocurrent generation going from  $C_{60}$  to  $C_{70}$  pyrrolidinofullerenes. Both  $C_{60}$ - and  $C_{70}$ -based PyFs demonstrated wide and quite intense interaction bands between 400 and 550 nm that contribute strongly to the photocurrent as revealed from the IPCE spectra.

It is also notable that the applied pyrrolidinofullerenes give quite different open circuit voltages in solar cells with ZnPC; the  $V_{oc}$  varies from  $\sim 420$  mV for PyF-1/ZnPC to  $\sim 600$  mV for PyF-3/ZnPC devices. It is known that the open circuit voltage in organic solar cells is determined mostly by the energy difference between the acceptor LUMO and donor HOMO levels.<sup>13,33</sup> The LUMO level energies of PyFs 1–5 and PCBM are very similar because the first reduction potentials of these compounds do not differ by more than 40 mV (see above, Table 1). The energies of the LUMO level of PCBM and HOMO level of ZnPC were estimated previously as ca.  $-4.3$  and  $-5.3$  eV, respectively.<sup>13,39</sup> Therefore, the maximal  $V_{oc}$  value achievable in bilayer solar cells comprising PCBM and ZnPC should be around 1.0 V. The experimental  $V_{oc}$  values obtained in this work are lower

(38) El-Khouly, M. E.; Ito, O.; Smith, P. M.; D'Souza, F. *J. Photochem. Photobiol., C* **2004**, *5*, 79.

(39) Gao, W.; Kahn, A. *Appl. Phys. Lett.* **2001**, *79*, 4040.

(Table 2) that evidences external effects such as an existence of interfacial barriers at the electrodes and, most probably, also between the layers of photoactive materials. A relatively low  $V_{oc}$  (<500 mV) is the most important drawback of the  $C_{60}$ /ZnPc solar cells that can generate very high currents due to the low energy gap of the phthalocyanine.<sup>25,27</sup> However, the energy levels of these materials allow for a  $V_{oc}$  as high as  $\sim 1000$  mV. Further investigation of PyF materials in various organic solar cell architectures might further increase the  $V_{oc}$  and therefore the efficiency of these solar cells.

**Multicomponent Organic Solar Cells Fabricated from PyFs, the Polyconjugated Polymer MDMO-PPV, and ZnPc.** *Device Architecture and Working Principle.* The MDMO-PPV/PCBM bulk heterojunction solar cells collect the sunlight in a spectral region between 350 and 600 nm, whereas the major fraction of the photocurrent produced by bilayer fullerene/ZnPc devices comes from the wide Q-band absorption of ZnPc at 580–800 nm. This is illustrated by the active layer absorption and IPCE spectra for PCBM/MDMO-PPV and PyF-2/ZnPc photovoltaic cells (Figure 6). Therefore, it looks very promising to combine both types of cells in one device to achieve photocurrent generation over a wide spectral region. One way to do so is to combine both cell concepts via a recombination contact to produce an organic tandem device, the feasibility of which was shown recently.<sup>40,41</sup> In the following, a more direct approach utilizing the interaction between ZnPc and PyF is presented.

The devices were fabricated by spin-coating a blend of fullerene derivatives and MDMO-PPV on vacuum-evaporated ZnPc films. The schematic layout of such a multicomponent solar cell is shown in Figure 7. The best results were obtained when a mixture of PCBM with a small amount of pyrrolidinofullerene **3** was used as acceptor material (Table 3). The choice of this pyrrolidinofullerene was motivated by two main factors. First, PyF-3 exhibited the best performance in diffusion bilayer devices compared with the other PyFs. Second, the first reduction potential of PyF-3 matches perfectly the first reduction potential of PCBM (Table 1), indicating that both compounds have very similar electron affinities. Therefore, the addition of small amounts of PyF-3 to PCBM should not affect significantly the electron transport properties of the material.

The proposed working mechanism of the multicomponent cells is absorption of light mainly in the phthalocyanine and polymer phase of the solar cell with subsequent dissociation of the excitation at the nearest interface to a fullerene. The electrons are transported to the aluminum back electrode via the fullerene phase while the holes generated in the polymer can move through the ZnPc layer to the ITO/PEDOT (indium tin oxide/poly(3,4-ethylenedioxy)thiophene) electrode. The rather good fill factor of the best devices fabricated (>50%) shows that the transport over the ZnPc layer is not severely limiting the performance of the multicomponent solar cells. The higher lying hole transport level of the ZnPc results in

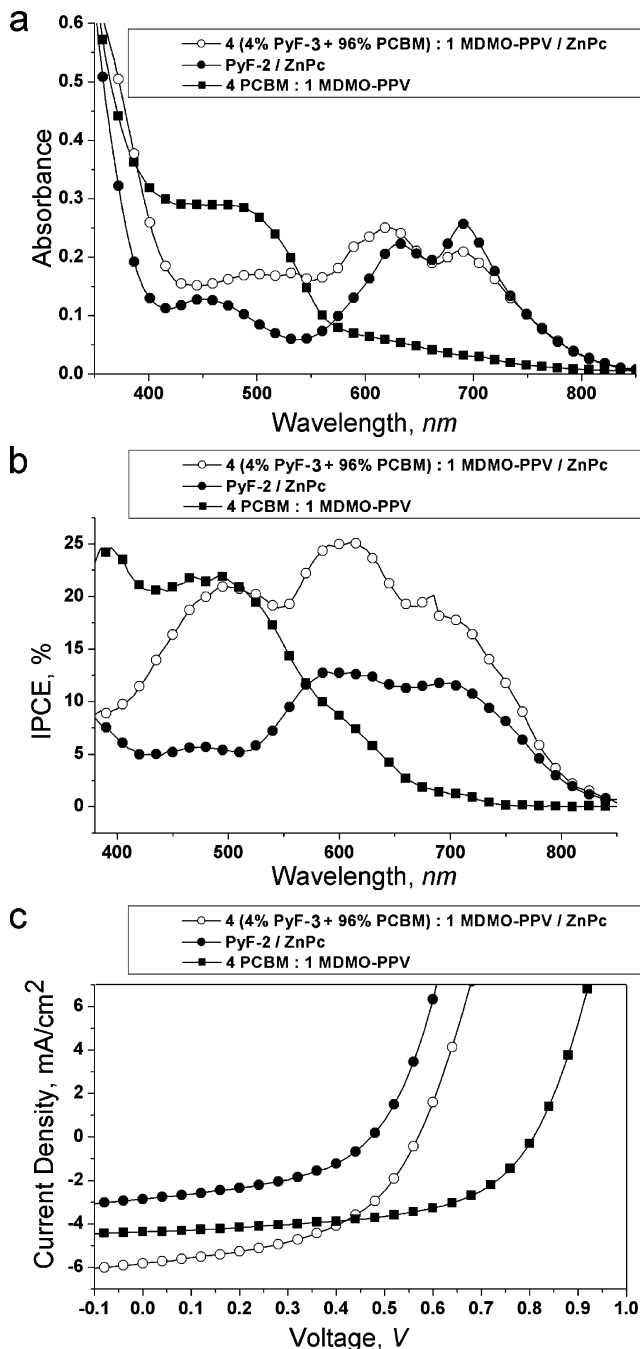


**Figure 6.** Active layer absorption (a) and IPCE (b) spectra of the bulk heterojunction PCBM/MDMO-PPV, diffusion bilayer PyF/ZnPc, and multicomponent solar cells shown together with the corresponding linear  $I$ - $V$  curves (c).

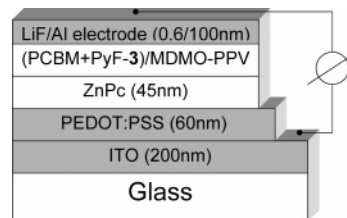


**Figure 7.** Schematic layout of the investigated multicomponent solar cell architecture. To obtain such devices, the bulk heterojunction layer comprising two fullerene derivatives (PyF and PCBM) and polymer MDMO-PPV was spin-coated from chlorobenzene on the top of the evaporated ZnPc film.

a significantly lower  $V_{oc}$  than in MDMO-PPV/PCBM solar cells,<sup>33</sup> which is the biggest drawback of this concept. A

(40) Dennler, G.; Prall, H. J.; Koeppel, R.; Egginger, M.; Autengruber, R.; Sariciftci, N. S. *Appl. Phys. Lett.* **2006**, *89*, 073502.

(41) Hadipour, A.; Boer, B.; Wildeman, J.; Kooistra, F. B.; Hummelen, J. C.; Turbiez, M. G. R.; Wienk, M. M.; Janssen, R. A. J.; Blom, P. W. M. *Adv. Funct. Mater.* **2006**, *16*, 1897.

**Table 3. Output Parameters of Multicomponent Solar Cells Fabricated under Different Conditions**

composition of the acceptor phase	solvent <sup>a</sup>	ZnPc				
		thickness, nm	$V_{oc}$ , mV	$I_{sc}$ , mA/cm <sup>2</sup>	FF, %	$\eta$ , %
100% PCBM	CB	45	515	3.2	53	0.8
2% PyF-3 + 98% PCBM	CB	45	560	5.0	52	1.5
4% PyF-3 + 96% PCBM	CB	45	570	5.75	50	1.6
8% PyF-3 + 92% PCBM	CB	45	540	5.0	51	1.4
16% PyF-3 + 84% PCBM	CB	45	530	3.7	43	0.8
33% PyF-3 + 67% PCBM	CB	45	490	3.8	43	0.8
67% PyF-3 + 33% PCBM	CB	45	310	0.5	33	0.05
100% PyF-3	CB	45	310	0.25	23	0.01
4% PyF-3 + 96% PCBM	CF	45	460	0.9	27	0.11
4% PyF-3 + 96% PCBM	DCM	45	420	0.6	28	0.07
4% PyF-3 + 96% PCBM	CB	30	500	4.3	44	0.9
4% PyF-3 + 96% PCBM	CB	60	470	4.7	51	1.1
4% PyF-4 + 96% [70]PCPP	DCB	45	590	7.3	48	2.1

<sup>a</sup> CB stands for chlorobenzene, CF for chloroform, DCM for dichloromethane, and DCB for 1,2-dichlorobenzene.

better suited material combination with less different energy levels might reduce this loss.

**Performance of the Multicomponent Solar Cells.** The active layer absorption covers the whole visible region (350–800 nm); moreover, this absorption generates photocurrent concluded from the IPCE spectra of the devices (Figure 6b). The best multicomponent solar cells produce photocurrent densities of up to 6.0 mA/cm<sup>2</sup>; this is higher than the  $I_{sc}$  of MDMO–PPV/PCBM or PyF/ZnPc solar cells (Figure 6c). The open circuit voltage and fill factor values are somewhat lower (570 mV and 50%, respectively) than for MDMO–PPV/PCBM bulk heterojunction solar cells; therefore, the best multicomponent cells investigated in this work yield solar power conversion efficiencies of 1.6–1.7% competitive to low energy gap polymers that collect the sun light in the same region.<sup>18,19</sup>

Further optimization of the material composition and device fabrication conditions might lead to higher performances. For example, the application of C<sub>70</sub>-based fullerene materials attempted in this work, namely, the methanofullerene [70]PCPP (Figure 1) and PyF-4 (Scheme 1), raised the photocurrent to 7.3 mA/cm<sup>2</sup> and power conversion efficiency to 2.1% (Table 3). This increase in the photocurrent arises from the stronger absorption of C<sub>70</sub> derivatives in the visible range, an effect described previously for conventional bulk heterojunction solar cells.

**ZnPc Film Thickness and Solvent Effects.** The optimal thickness of the ZnPc bottom layer is about 45 nm for solar cells investigated in this work, while devices with 30 and 60 nm films of ZnPc give a worse performance (Table 3). Several different solvents were tested for deposition of the fullerene/polymer blends on the ZnPc layer; the efficiency of the resulting solar cells decreases in the order chlorobenzene  $\gg$  chloroform  $\approx$  dichloromethane. A similar solvent effect was observed for the conventional bulk heterojunction MDMO–PPV/PCBM solar cells.<sup>9</sup> A number of previous studies showed that the choice of solvent strongly affects the active layer morphology and the use of chlorobenzene as a solvent gives the best results.<sup>4</sup> In the case of the multicomponent cells, the atomic force microscopy (AFM) images showed that the nanomorphology of the top fullerene (mix of 4% PyF and 96% PCBM)–polymer layer is

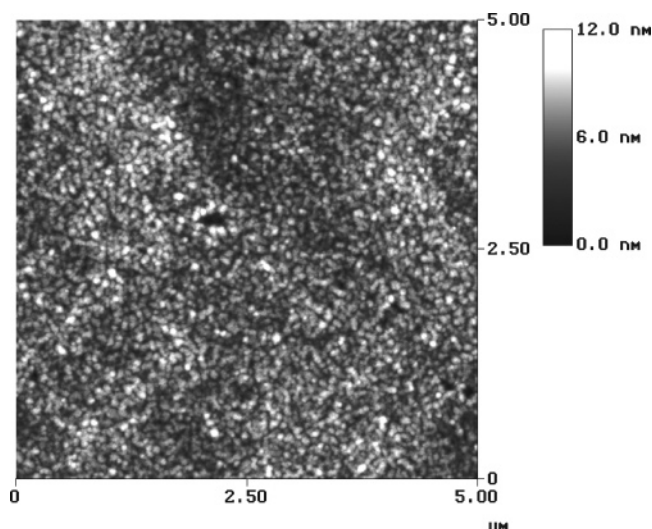


**Figure 8.** AFM image of a 4 (4% PyF-3 + 96% PCBM)/1 MDMO–PPV blend film spin-coated on 45 nm ZnPC bottom layer.

comparable to the morphology of the PCBM/MDMO–PPV films with good solar cell performances (Figure 8).<sup>9</sup> Thus, the bottom ZnPc layer seems to have no strong influence on the degree of the phase separation occurring in the fullerene/polymer layer deposited on the top.

**Effect of the PyF-3/PCBM Ratio.** An important factor that strongly influences the solar cell performance is the loading of the acceptor phase with PyF-3; the composition of the acceptor phase is expressed below by the weight percent ratios between PCBM and PyF-3. For instance, the solar cells fabricated using just pure PCBM as acceptor material showed relatively low performance (Table 3). However, the introduction of even very small amounts of PyF-3 to the PCBM/MDMO–PPV blend (2% of PyF-3 with respect to 98% of PCBM) significantly improves the power conversion efficiency. The overall dependence of the solar cell parameters on the PyF-3–PCBM ratio is illustrated on the diagrams in Figure 9. An acceptor material comprising 4% of PyF-3 with 96% of PCBM gives the best solar cell parameters. Following the increase in the content of PyF-3 and decrease in the content of PCBM in the blend leads again to lower solar cell efficiencies. It is notable that both  $V_{oc}$  and  $I_{sc}$  are similarly affected by the pyrrolidinofullerene content, while the fill factor is less sensitive but still obeys the same trend.

We presume that such drastic change of the solar cell performance upon addition of PyF-3 is connected to the supramolecular interaction between the compounds in the studied multicomponent systems. Most likely, it is the complex formation between PyF-3 and ZnPc at the interphase between the photoactive materials mentioned before. To verify this, we investigated the change of the active layer absorption and the IPCE spectra of photovoltaic devices with different PyF loading.

The active layer absorption spectra (Figure 10a) show the same tendency as in the ZnPc–PyF bilayer devices. Addition of PyF leads to a shifting and narrowing of the Q-band double-peak spectrum which intensifies with the amount of PyF added to the solution spin-cast on top of the ZnPc layer. This indicates that the complexation is also occurring in these devices.

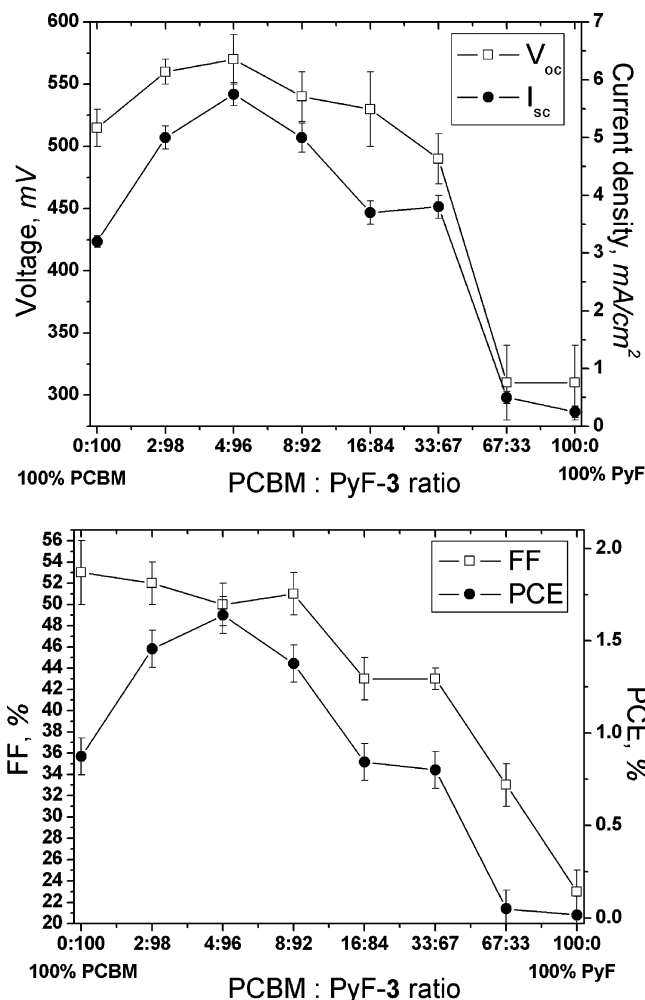


**Figure 9.** Dependence of the solar cell output parameters on the PyF/PCBM ratio used for their fabrication.

The photocurrent action spectra (IPCE) of the multicomponent solar cells also exhibit a very strong dependence on the ratio between PyF-3 and PCBM used as acceptor materials (Figure 10b). Thus, solar cells made using just PCBM without addition of PyF-3 produce photocurrent mainly in the 350–580 nm spectral region (like conventional PCBM/MDMO-PPV bulk heterojunction devices), whereas the contribution from the phthalocyanine absorption (580–800 nm region) is much weaker. The addition of small amounts of PyF-3 (2% of PyF-3 with respect to 98% of PCBM) changes the situation remarkably: the intensity of the 580–800 nm features increases by a factor of 2.5 up to the same intensity as the 350–580 nm part of the IPCE spectrum. At the same time, the addition of 2% of PyF-3 nearly doubles the solar cell power conversion efficiency as seen from the  $I$ - $V$  measurements (Table 3).

The positive influence of PyF on the efficiency of solar cells stops at the component ratio 8% of PyF-3 to 92% of PCBM; above that the 350–550 nm part of IPCE spectrum becomes rather weak, indicating a lower contribution from MDMO-PPV and PCBM to the current generation. This effect becomes even more pronounced when the content of PyF-3 reaches 16% and 33% (with respect to 84% and 67% of PCBM). The IPCE spectrum of the devices made using a combination of 33% of PyF-3 with 67% of PCBM looks like the typical spectrum of bilayer PyF/ZnPc solar cells

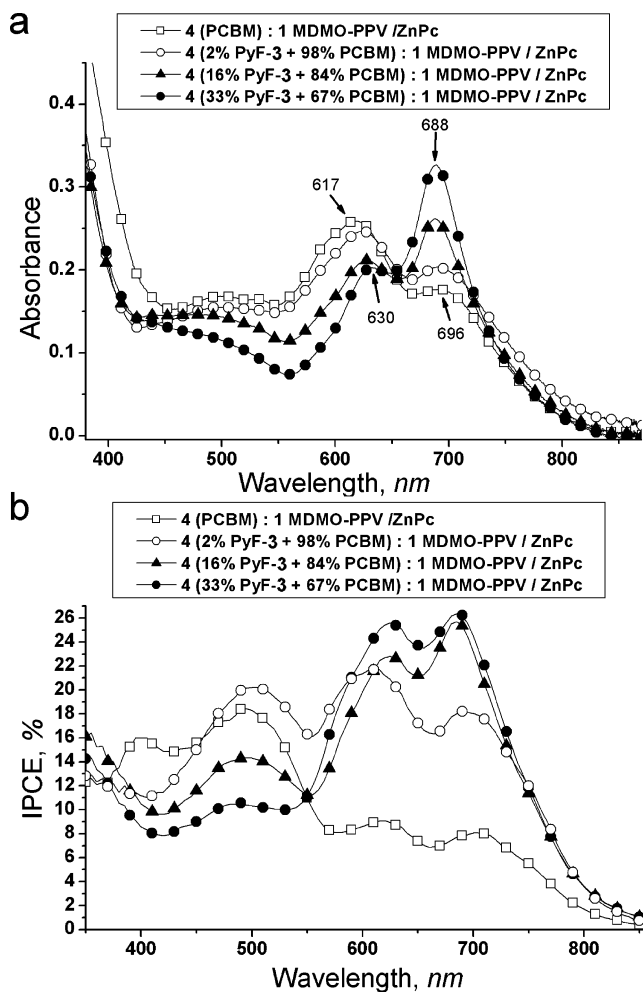


**Figure 10.** Influence of the PyF-3 loading on the active layer absorption (a) and IPCE (b) spectra of multicomponent devices.

(Figure 10b); this means that MDMO-PPV does not contribute significantly to the photocurrent in this case. Presumably, 33% of PyF-3 is enough to block the phthalocyanine surface entirely via the complex formation. Then the layer of the ZnPc-PyF-3 complexes separates phthalocyanine and MDMO-PPV phases blocking the hole transport from the polymer to the ITO electrode. On the other hand, electron transport is not seriously affected: the PyF-3 complexed with ZnPc still has some communication with the fullerene-rich phase in the fullerene/polymer blend.

In summary, multicomponent organic solar cells made from MDMO-PPV, ZnPc, PCBM, and PyF-3 exhibit good performance and efficient photocurrent generation in a wide spectral region. The content of the pyrrolidinofullerene **3** in the active layer of the solar cell is a crucial factor that strongly influences the device performance; an optimal PCBM/PyF-3 ratio must be found to achieve the maximum photocurrent generation from both blue- and red-absorbing materials.

### 3. Conclusions

We investigated interactions between five different pyrrolidinofullerenes bearing chelating pyridyl groups (PyFs) and ZnPc in solid-state thin films. Absorption measurements indicated a coordination complex formation between PyF and

ZnPc layers. This complexation of ZnPc and PyF proposed to improve the performance of organic solar cells fabricated from these materials. PyF–ZnPc solar cells reach power conversion efficiencies of up to 1.5% in this study; this value is nearly 3 times higher as compared to the nonchelating reference system PCBM–ZnPc.

Novel multicomponent organic solar cells were made by spin-coating a blend of fullerene/MDMO–PPV on evaporated ZnPc films. The performance of solar cells with pure PCBM as the fullerene phase in the bulk heterojunction is quite low (<1%); however, the addition of small amounts of PyF to the PCBM (ratio 2%/98%, respectively) doubles the power conversion efficiency. Introduction of PyF into the fullerene phase strongly increases the photocurrent generation in the 600–800 nm spectral region (corresponding to the ZnPc Q-band absorption) due to the complex formation between PyF and ZnPc.

It seems that the combination of bilayer fullerene/ZnPc and bulk heterojunction fullerene/polymer photovoltaic devices can be considered a promising approach to achieve a wide spectral response in organic solar cells while retaining the good charge-transfer and transport properties of established materials. The already achieved PCE of 2.1% is on the level of the best reported to date low band gap polymer systems.

#### 4. Experimental Section

**Materials and Instrumentation.** All reagents and solvents were purchased from Acros Organics and used as received except for a special grade dichloromethane from Aldrich. Zinc phthalocyanine was obtained from Chemos GmbH and purified by recrystallization after vacuum sublimation. PCBM (99.5+) was purchased from Nano C.

The absorption spectra were recorded with a Varian 3G UV–vis spectrophotometer. The photocurrent spectra were measured with a SRS 830 lock-in amplifier using the monochromated light from a 75 W Xe lamp as excitation. *I*–*V* characteristics were recorded using a Keithley 236 source meter, illumination was provided by a KHS Steuernagel solar simulator calibrated to correspond to 100 mW/cm<sup>2</sup> at AM1.5.

**Synthesis of the Fullerene Derivatives.** Compounds **1** (*cis*-2',5'-di(pyridin-3-yl)pyrrolidino[3',4':1,9](C<sub>60</sub>-I<sub>h</sub>)[5,6]fullerene) and **2** (*trans*-1'-((pyridin-3-yl)methyl)-2',5'-di(pyridin-3-yl)pyrrolidino[3',4':1,9](C<sub>60</sub>-I<sub>h</sub>)[5,6]fullerene) were prepared according to the previously published procedure.

Pyrrolidinofullerene **3** (*trans*-1'-((pyridin-3-yl)methyl)-2',5'-di(pyridin-2-yl)pyrrolidino[3',4':1,9](C<sub>60</sub>-I<sub>h</sub>)[5,6]fullerene) was prepared by heating at reflux C<sub>60</sub> (1.00 g, 1.39 mmol), 2-picolyl-3-picolylamine (333 mg, 1.67 mmol), and 2-pyridinecarboxaldehyde (0.2 mL, 2.10 mmol) in 1,2-dichlorobenzene (150 mL) for 10 min. The chromatographic separation (silica gel, 30–75 μm, 90 Å, eluent toluene–MeOH 98.0:2.0 v/v) resulted in isolation of **3** as pure *trans* isomer (yield 813 mg, 58%). <sup>1</sup>H NMR (CDCl<sub>3</sub>, 400 MHz) δ = 3.80 (d, 1H), 4.39 (d, 1H), 6.80 (br s, 2H), 7.31 (dt, 2H), 7.45 (dd, 1H), 7.72 (br s, 2H), 7.77 (t, 2H), 8.00 (d, 1H), 8.66 (dd, 1H), 8.75 (d, 1H), 8.88 (br s, 2H) ppm. <sup>13</sup>C NMR (CS<sub>2</sub>–(CD<sub>3</sub>)<sub>2</sub>CO 9:1, 150 MHz): 48.85, 74.28, 76.42, 78.24, 122.94, 123.57, 124.73, 133.73, 135.53, 136.39, 136.58, 137.41, 139.50, 139.95, 141.56, 141.83, 141.92, 142.09, 142.17, 142.29, 142.55, 142.65, 143.13, 144.58, 144.63, 145.14, 145.16, 145.25, 145.54, 145.67, 145.96, 146.00, 146.05, 146.22, 146.26, 146.56, 147.33, 148.98, 149.91, 150.03, 153.65, 156.01, 159.31 ppm.

Pyrrolidinofullerene **4** (*trans*-1'-((pyridin-3-yl)methyl)-2',5'-di(pyridin-2-yl)pyrrolidino[3',4':8,25](C<sub>70</sub>-D<sub>5h(6)</sub>)[5,6]fullerene) was synthesized by treatment of C<sub>70</sub> (300 mg, 0.36 mmol) with 2-picolyl-3-picolylamine (78.8 mg, 0.39 mmol) and 2-pyridinecarboxaldehyde (0.1 mL, 1.05 mmol) at reflux in 1,2-dichlorobenzene (50 mL) for 10 min (Scheme 1). The chromatographic separation (silica gel, 40–60 μm, 60 Å, eluent toluene–MeOH 97.5:2.5 v/v) resulted in isolation of isomerically pure product **4** with 45% yield. <sup>1</sup>H NMR (CS<sub>2</sub>–(CD<sub>3</sub>)<sub>2</sub>CO 9:1, 400 MHz) δ = 3.36 (d, 1H), 4.04 (d, 1H), 5.82 (s, 1H), 6.25 (s, 1H), 7.30 (m, 2H), 7.62 (t, 1H), 7.71 (d, 1H), 7.80 (d, 1H), 7.90 (t, 1H), 8.35 (s, 1H), 8.48 (m, 2H), 8.70 (d, 1H), 8.83 (m, 1H), 8.91 (d, 1H) ppm. <sup>13</sup>C NMR (CS<sub>2</sub>–(CD<sub>3</sub>)<sub>2</sub>CO 9:1, 150 MHz): 48.19, 66.57, 67.67, 72.68, 76.63, 122.89, 123.06, 123.45, 123.63, 124.39, 124.73, 124.93, 125.55, 127.84, 128.42, 129.14, 130.64, 131.18, 131.23, 131.30, 131.73, 132.97, 133.10, 133.43, 133.70, 133.79, 135.34, 136.19, 136.35, 136.50, 137.40, 137.44, 138.64, 140.37, 140.73, 142.82, 142.87, 143.15, 143.19, 143.24, 143.34, 145.69, 145.79, 146.04, 146.25, 146.40, 146.83, 147.04, 147.09, 147.33, 147.45, 147.51, 148.79, 148.89, 148.97, 149.06, 149.11, 149.26, 149.42, 149.57, 149.69, 149.91, 150.06, 150.45, 150.53, 150.63, 150.72, 151.00, 151.37, 151.42, 151.48, 155.15, 157.22, 159.06, 159.24, 159.76 ppm.

For preparation of **5** (a mixture of *cis*-2',5'-di(pyridin-3-yl)pyrrolidino[3',4':8,25](C<sub>70</sub>-D<sub>5h(6)</sub>)[5,6]fullerene and *cis*-2',5'-di(pyridin-3-yl)pyrrolidino[3',4':9,10](C<sub>70</sub>-D<sub>5h(6)</sub>)[5,6]fullerene) fullerene C<sub>70</sub> (300 mg, 0.36 mmol) was heated at reflux with 3-picolylamine (50.2 mg, 0.46 mmol), 3-pyridinecarboxaldehyde (0.1 mL, 1.05 mmol), and butyric acid (2 mL) in 1,2-dichlorobenzene (50 mL) for 12 h (Scheme 1). Following the chromatographic separation (silica gel, 40–60 μm, 60 Å, eluent toluene–MeOH 98:2 v/v) gave **5** as a mixture of two isomers with 38% yield. <sup>1</sup>H NMR (CDCl<sub>3</sub>, 400 MHz) δ = 2.06 (broad s, ~1H, 5,6 isomer), 2.85, (broad s, 1H, 1,2-isomer), 4.88 (s, ~1H, 5,6 isomer), 5.19 (d, 1H, 1,2-isomer), 5.35 (s, 1H, 1,2-isomer), 7.31 (dt, 1H, 1,2-isomer), 7.38 (dt, ~1H, 5,6-isomer), 7.63 (dt, 1H, 1,2-isomer), 7.71 (d, ~1H, 5,6-isomer), 8.15 (d, 1H, 1,2-isomer), 8.20 (d, ~1H, 5,6-isomer), 8.56 (d, 1H, 1,2-isomer), 8.68 (d, 1H, 1,2-isomer), 8.85 (d, 1H, 1,2-isomer), 8.92 (s, ~1H, 5,6-isomer), 8.95 (s, 1H, 1,2-isomer), 9.33 (s, 1H, 1,2-isomer) ppm.

Methanofullerene [70]PCPP (3'-(phenyl)-3'-((2-(propoxycarbonyl)ethyl)-cyclopropa[8,25](C<sub>70</sub>-D<sub>5h(6)</sub>)[5,6]fullerene) was prepared from C<sub>70</sub> and tosylhydrazone of *n*-propyl benzoylpropionate in complete accordance to the method reported previously for the preparation of [70]PCBM.<sup>31</sup> The content of the major 1,2-isomer shown in Figure 1 was estimated by <sup>1</sup>H NMR as ~90% that is higher than in the case of [70]PCBM; the remaining 10% corresponded to one out of two possible diastereomers of the minor 5,6-adduct (in contrast to synthesis of [70]PCBM where both diastereoisomers were observed). The obtained [70]PCPP as a ~9:1 mixture of two isomers was used in this work as material in organic solar cells without further separation.

<sup>1</sup>H NMR (CS<sub>2</sub>–(CD<sub>3</sub>)<sub>2</sub>CO 9:1, 400 MHz) δ = 0.88 (t, 0.3H), 1.00 (t, 3H), 1.52 (q, 0.2H), 1.67 (q, 2H), 2.39 (m, 0.4H), 2.73 (m, 4H), 3.77 (t, 0.2H), 4.00 (t, 2H), 7.44 (t, 1.1H), 7.52 (t, 2.2H), 7.79 (d, 0.1H), 7.91 (br d, 2H) ppm. <sup>13</sup>C NMR (CS<sub>2</sub>–(CD<sub>3</sub>)<sub>2</sub>CO 9:1, 150 MHz): 11.01, 22.71, 29.81, 30.26, 30.98, 35.19, 66.06, 69.70, 71.75, 128.33, 128.43, 128.72, 129.05, 130.44, 130.63, 130.71, 130.85, 131.62, 132.73, 133.73, 133.92, 136.65, 137.67, 138.61, 139.38, 140.22, 141.05, 141.29, 141.55, 141.77, 142.54, 142.66, 143.27, 143.34, 143.63, 143.70, 143.87, 143.89, 144.08, 144.52, 144.54, 145.48, 145.65, 145.82, 145.91, 146.03, 146.24, 146.78, 146.92, 147.31, 147.38, 147.41, 147.46, 147.65, 147.82, 148.08, 148.28, 148.34, 148.42, 148.46, 148.49, 148.56, 149.03, 149.07, 149.15, 149.28, 149.34, 150.42, 150.47, 150.72, 150.74,

151.03, 151.08, 151.38, 151.89, 152.11, 155.13, 155.81, 170.62 ppm.

**Cyclic Voltammetry Measurements.** The cyclic voltammetry measurements were performed for ca.  $1 \times 10^{-3}$  M solutions of the fullerene derivatives in rigorously dried 1,2-dichlorobenzene in a cell equipped with glassy carbon working electrode ( $d = 2$  mm<sup>2</sup>), platinum wires as counter electrode, and SCE (saturated calomel electrode) as a reference electrode. The scan rate was 200 mV/s. A 0.1 M solution of Bu<sub>4</sub>NPF<sub>6</sub> was used as supporting electrolyte.

**Preparation of Bilayer Fullerene/ZnPc Systems and Corresponding Photovoltaic Devices.** An ~60 nm thick film of poly-(3,4-ethylenedioxy)thiophene:poly(styrenesulfonate) (PEDOT:PSS) (Baytron P) was spin-cast on glass substrates (14 × 14 mm) coated with 200 nm indium tin oxide (ITO) and dried under vacuum prior to the deposition of ZnPc. Zinc phthalocyanine was sublimed in a Leybold Univex 350 evaporation chamber at a pressure below  $10^{-5}$  mbar to obtain films with 30–60 nm thickness. Fullerene derivatives were dissolved in dry special grade dichloromethane (Sure/Seal bottle from Aldrich) to achieve concentrations of 15 mg/mL. One drop of the solution was put on top of the ZnPc-coated substrate rotating at 8000 rpm. Deposition of the fullerene derivatives at significantly lower rotation speeds results in serious damaging of the ZnPc surface and poor reproducibility of the results. After spin-coating the fullerene layer, the samples were transferred im-

mediately to an argon glovebox; there the deposition of a LiF (ca. 0.6 nm)–Al (100 nm) electrode was carried out under vacuum  $10^{-6}$  mbar in an evaporation chamber integrated in the glovebox.

**Preparation of Multicomponent Solar Cells.** The preparation procedure is very similar to that described above for bilayer solar cells. The fullerene (26 mg of PCBM and PyF mixed in different ratios) and 6 mg of MDMO–PPV are dissolved in 1 mL of HPLC-grade chlorobenzene (25 mg of [70]PCPP and 5 mg of MDMO–PPV are dissolved in 1 mL of 1,2-dichlorobenzene) under stirring at 50 °C for 36 h. One drop of the resulting solution was put on the ZnPc film rotating at 8000 rpm. Vacuum deposition of ZnPc on PEDOT–PSS/ITO and evaporation of LiF–Al electrodes on the fullerene/polymer blend was performed as described above for bilayer cells.

**Acknowledgment.** This work was supported by the Russian Ministry of Science and Education (Contract 02.513.11.3206 and 02.513.11.3209), INTAS (04-83-3733), RFBR (07-03-01078), and the Russian Science Support Foundation as well as by the Austrian Science Foundation (FWF) and the European Union via the Molycell project.

CM071243U